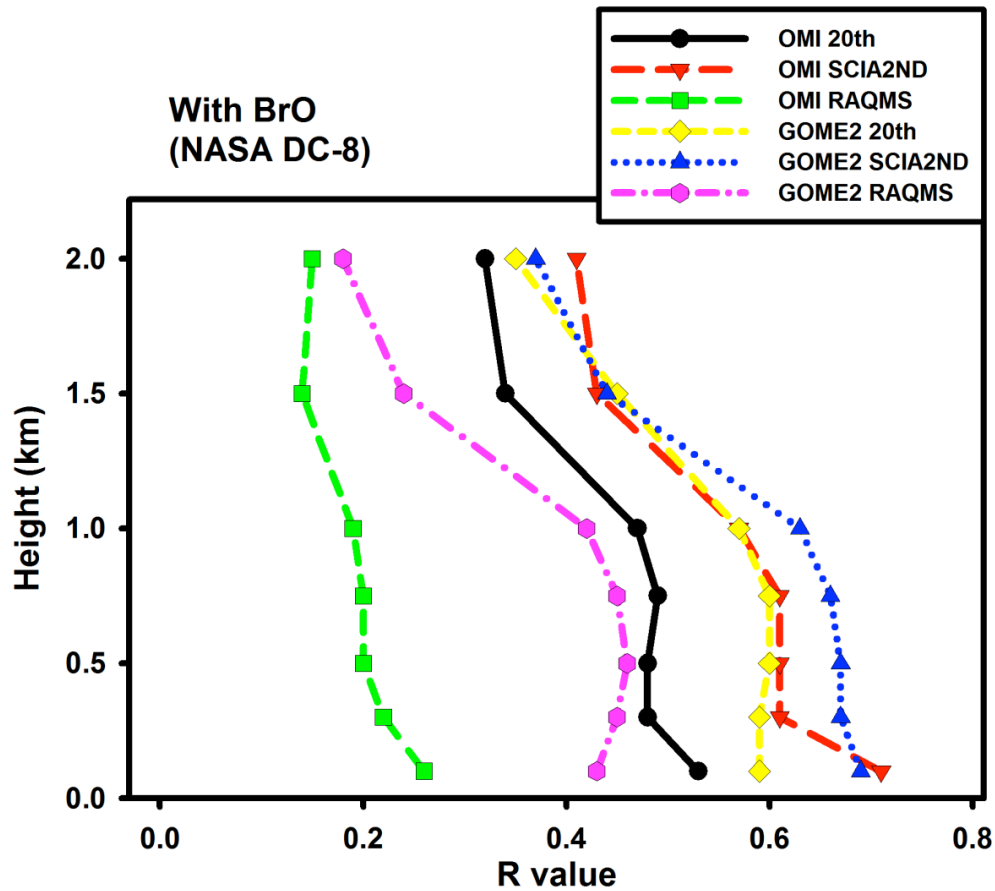


1
2
3
4
5
6
7
8
9
10
11
12
13
14
15
16
17
18
19
20
21
22

**Supplementary materials for : Characteristics of
tropospheric ozone depletion events in the Arctic
spring: Analysis of the ARCTAS, ARCPAC,
and ARCIONS measurements**

J.-H. Koo, Y. Wang, T. P. Kurosu, K. Chance,
A. Rozanov, A. Richter, S. J. Oltmans, A. M. Thompson,
J. W. Hair, M. A. Fenn, A. J. Weinheimer, T. B. Ryerson,
S. Solberg, L. G. Huey, J. Liao, J. E. Dibb, J. A. Newman,
J. B. Nowak, R. B. Pierce, M. Natarajan, and J. Al-saadi



24

25

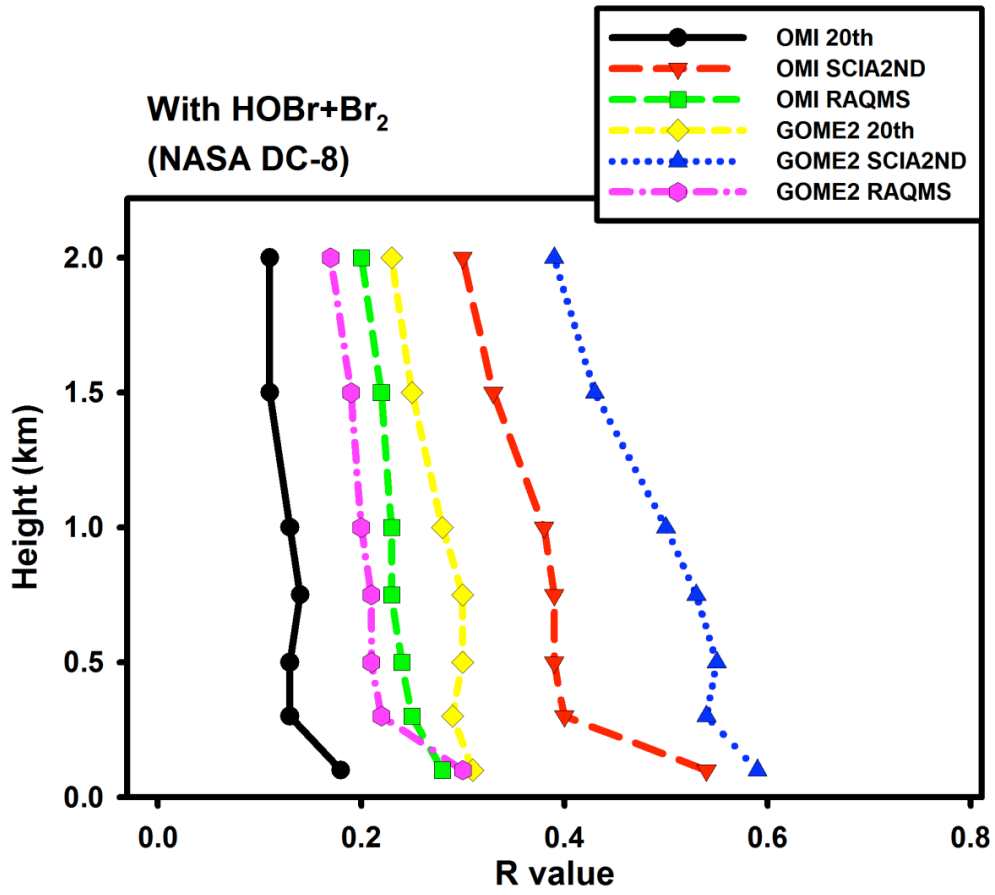
26 **Fig. S1.** Vertical profiles of correlation coefficients (R values) of retrieved tropospheric
 27 BrO columns with BrO measured from DC-8 Flights 9 and 10 (April 16 and 17). To
 28 correlate with tropospheric BrO columns with sufficient in situ data points, we integrate in
 29 situ aircraft observations of BrO, Br₂+HOBr, and soluble bromide from the surface to 7
 30 altitude levels (100, 300, 500, 750, 1000, 1500, and 2000 m). Tropospheric column BrO
 31 measurements corresponding to the in situ data points were sampled along the flight tracks.
 32 WP-3D data were not used because no significant correlation was found with column BrO;
 33 the reason is unclear. We used six tropospheric BrO VCD products, which are OMI-20th
 34 (black), OMI-SCIA2ND (red), OMI-RAQMS (green), GOME2-20th (yellow), GOME2-
 35 SCIA2ND (blue), and GOME2-RAQMS (purple).

36

37

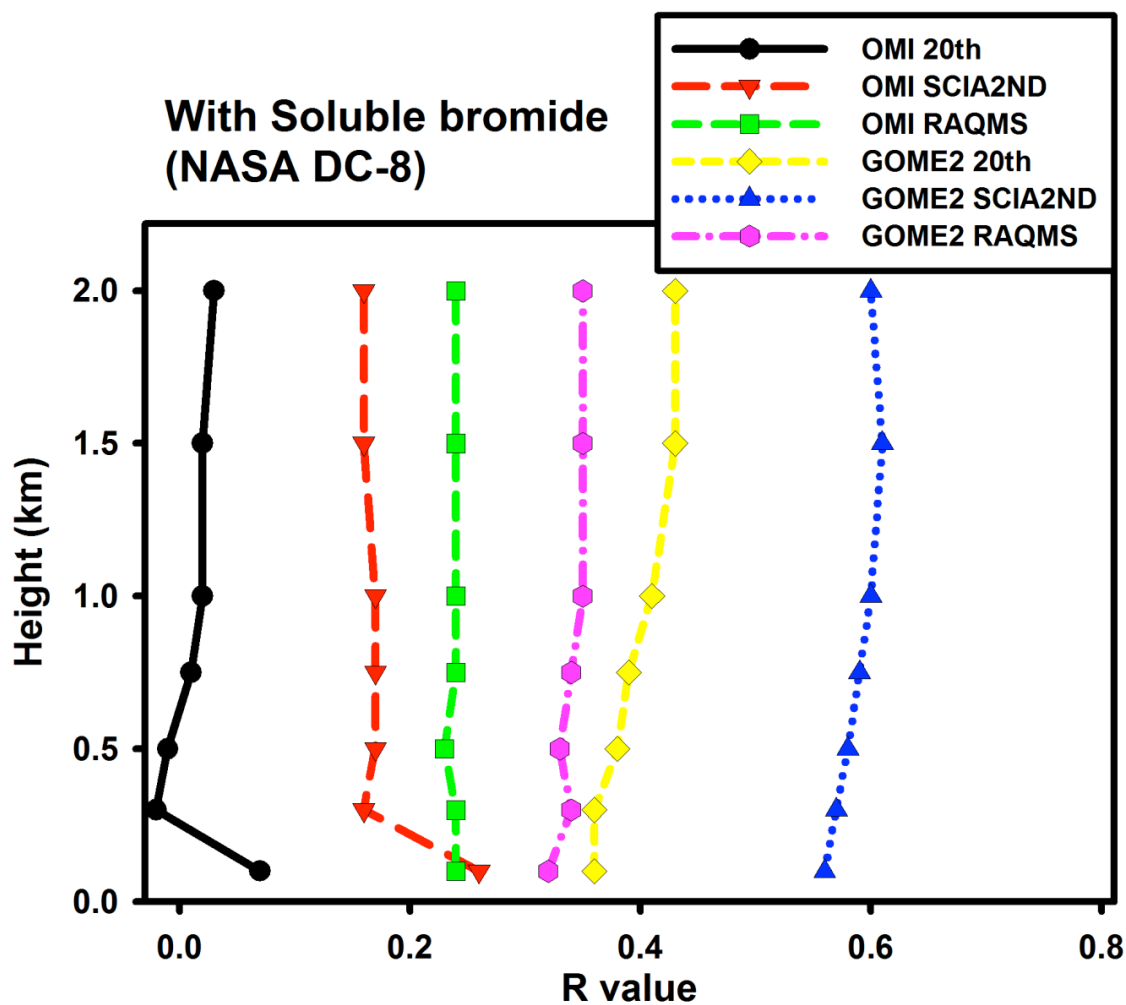
38

39



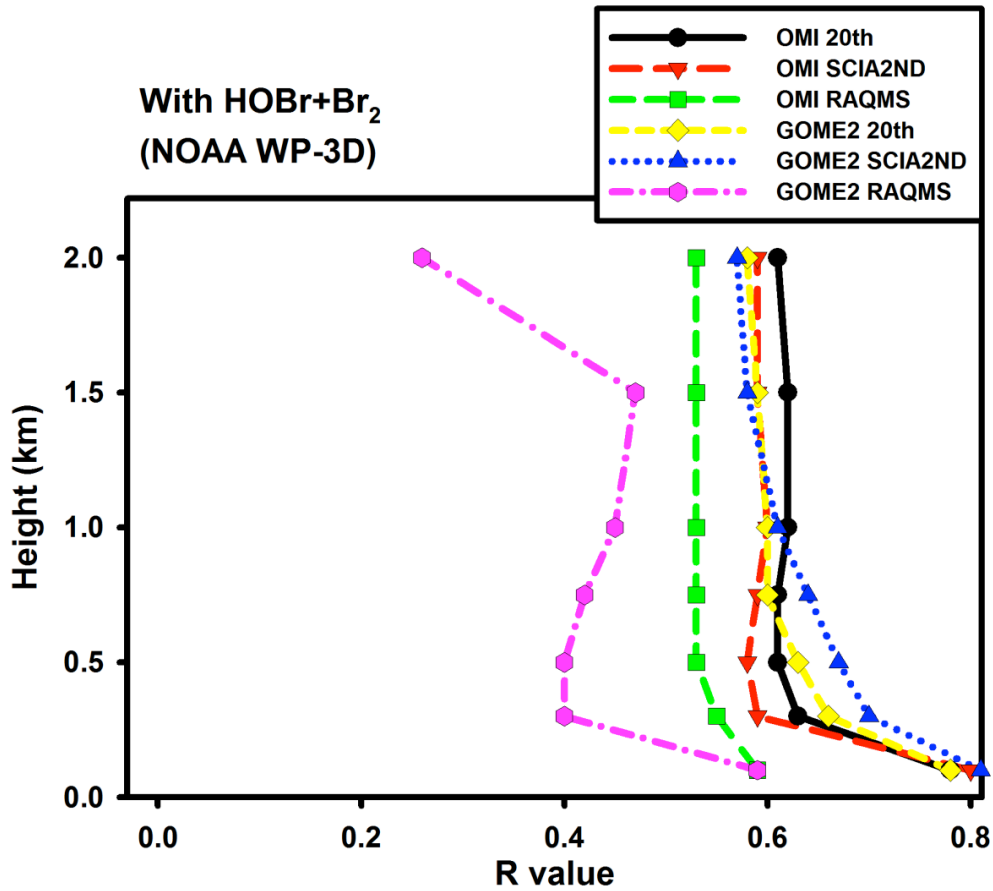
40
41
42
43
44
45
46
47
48
49
50
51
52
53
54

Fig. S2. Same as Fig. S1, but for correlations with integrated Br₂+HOBr in DC-8 flights (April 4, 5, 8, 9, 12, 16, and 17).



55
56
57
58
59
60
61
62
63
64
65
66
67
68
69

Fig. S3. Same as Fig. S2, but for correlations with integrated soluble bromide measured in DC-8 flights.



70

71

72 **Fig. S4.** Same as Fig. S1, but for correlations with integrated Br₂+HOBr in WP-3D flights
 73 (on April 12, 15, 18, 19, and 21). The more consistent correlation with Br₂+HOBr
 74 measurements during ARCPAC than ARCTAS (Fig. S2) reflects in part a smaller
 75 sampling region by WP-3D (to be shown in Fig. 5). The smaller sampling region leads to
 76 a smaller variation of the estimated stratospheric column BrO during ARCPAC than
 77 ARCTAS. The variation of tropospheric column BrO is therefore more consistent among
 78 the different products during ARCPAC than ARCTAS.

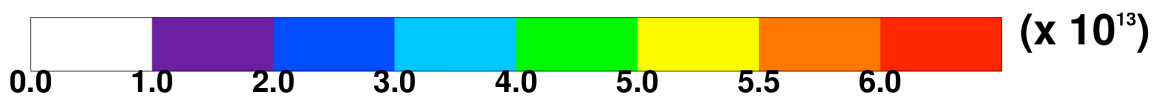
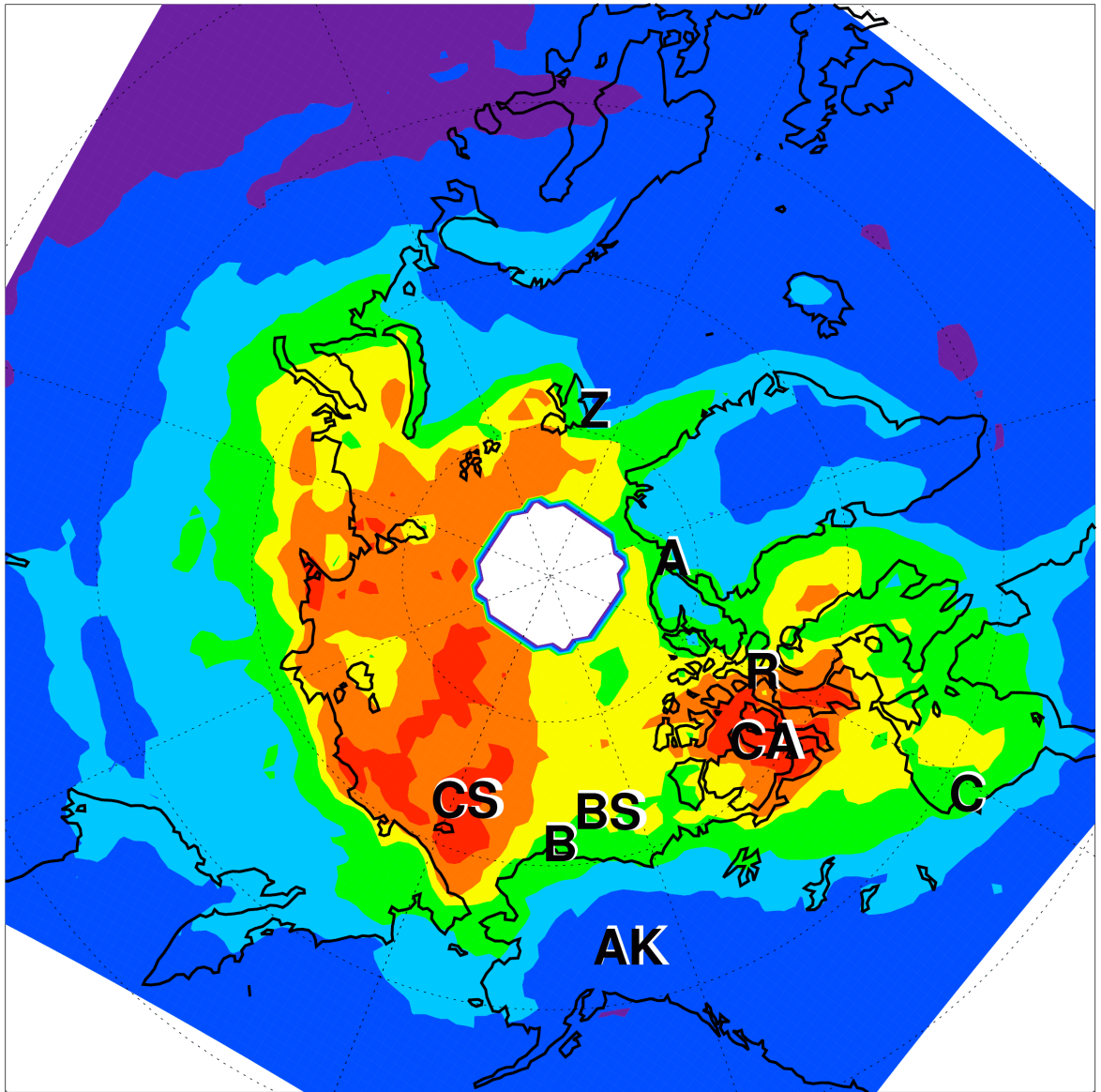
79

80

81

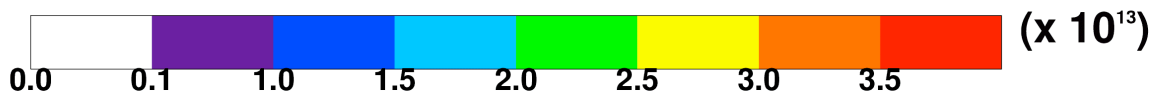
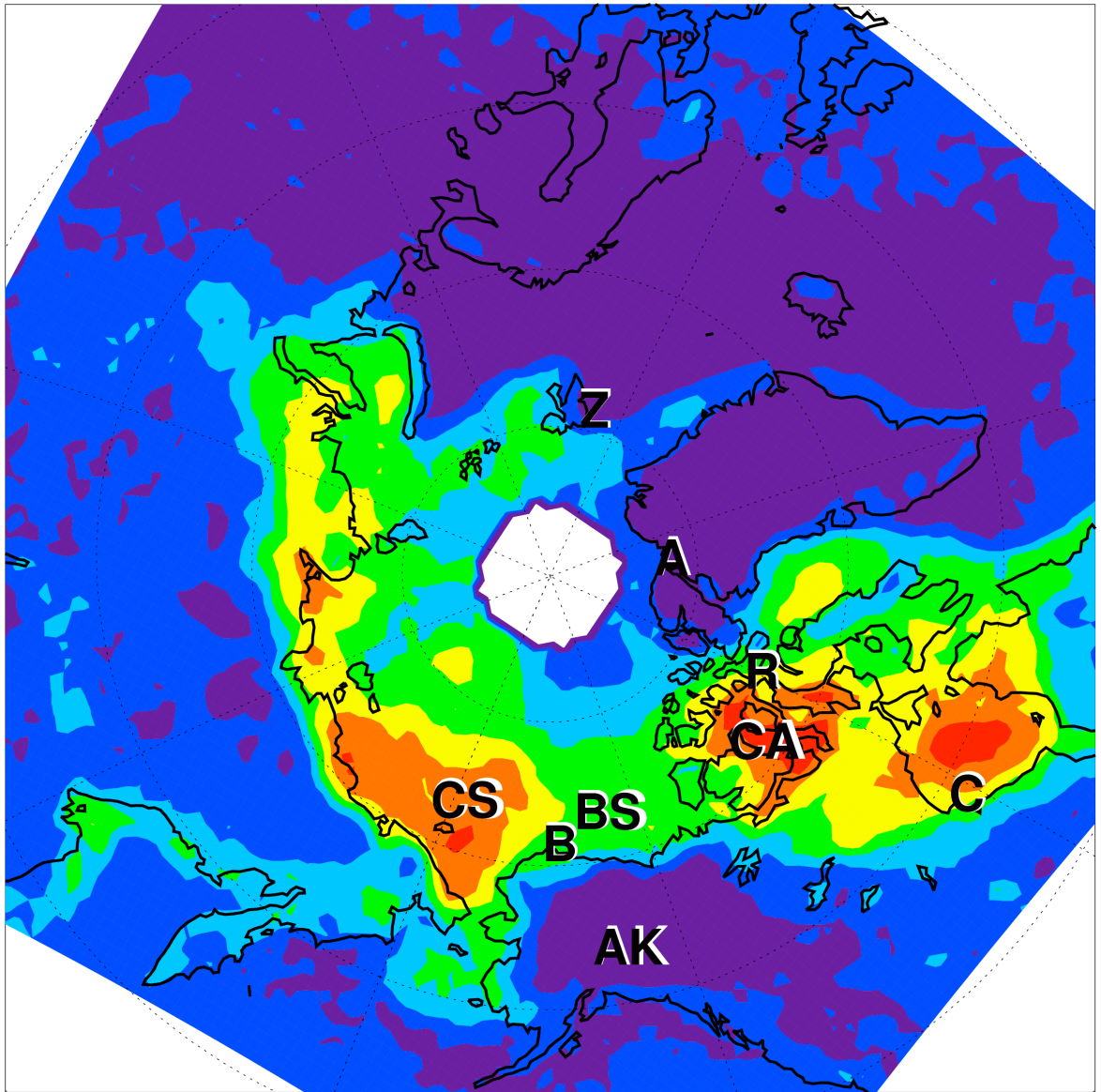
82

83



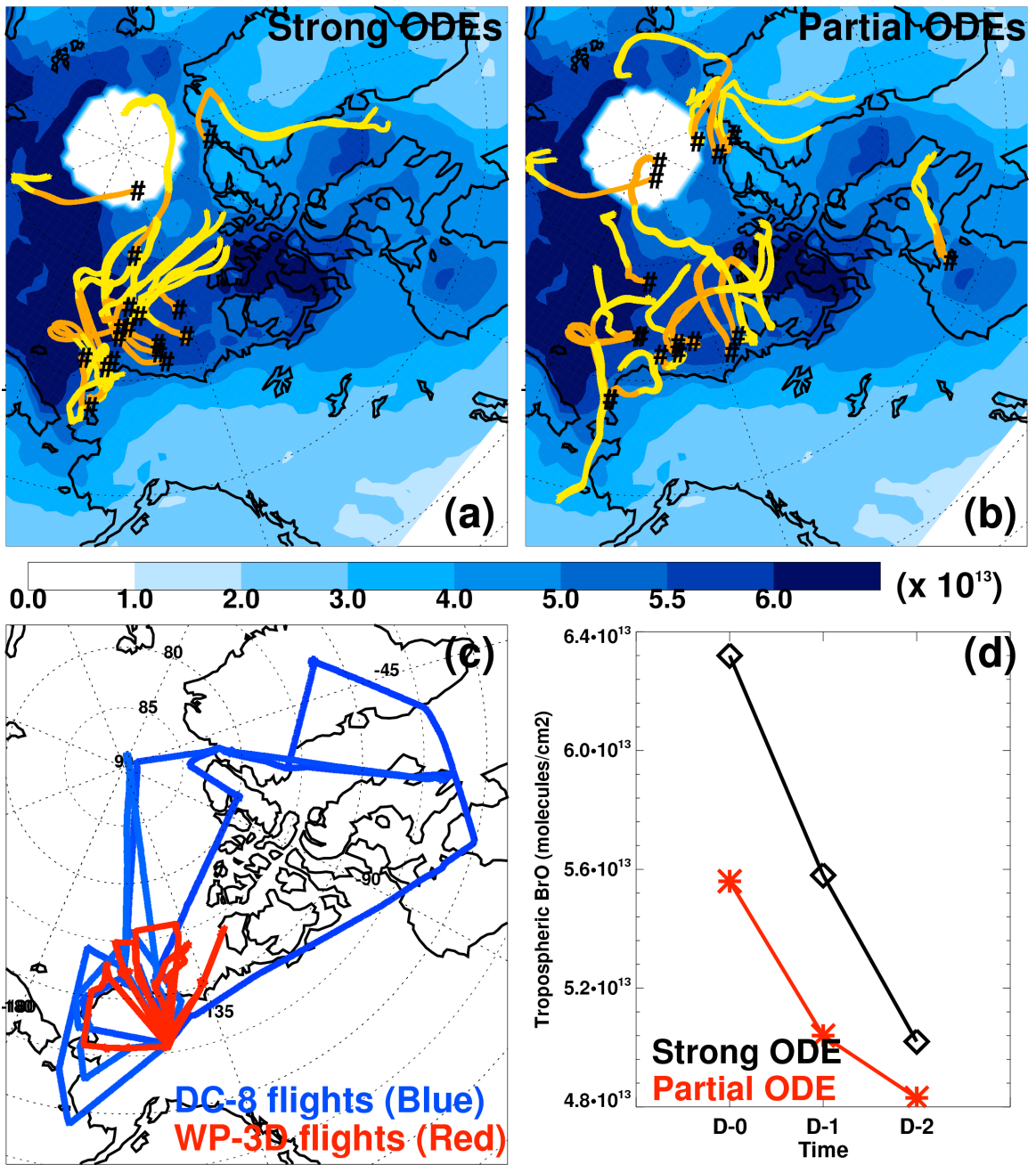
84
85
86
87
88
89
90
91
92
93

Fig. S5. Same as Fig. 2a, but for tropospheric BrO VCDs of OMI-SCIA2ND.



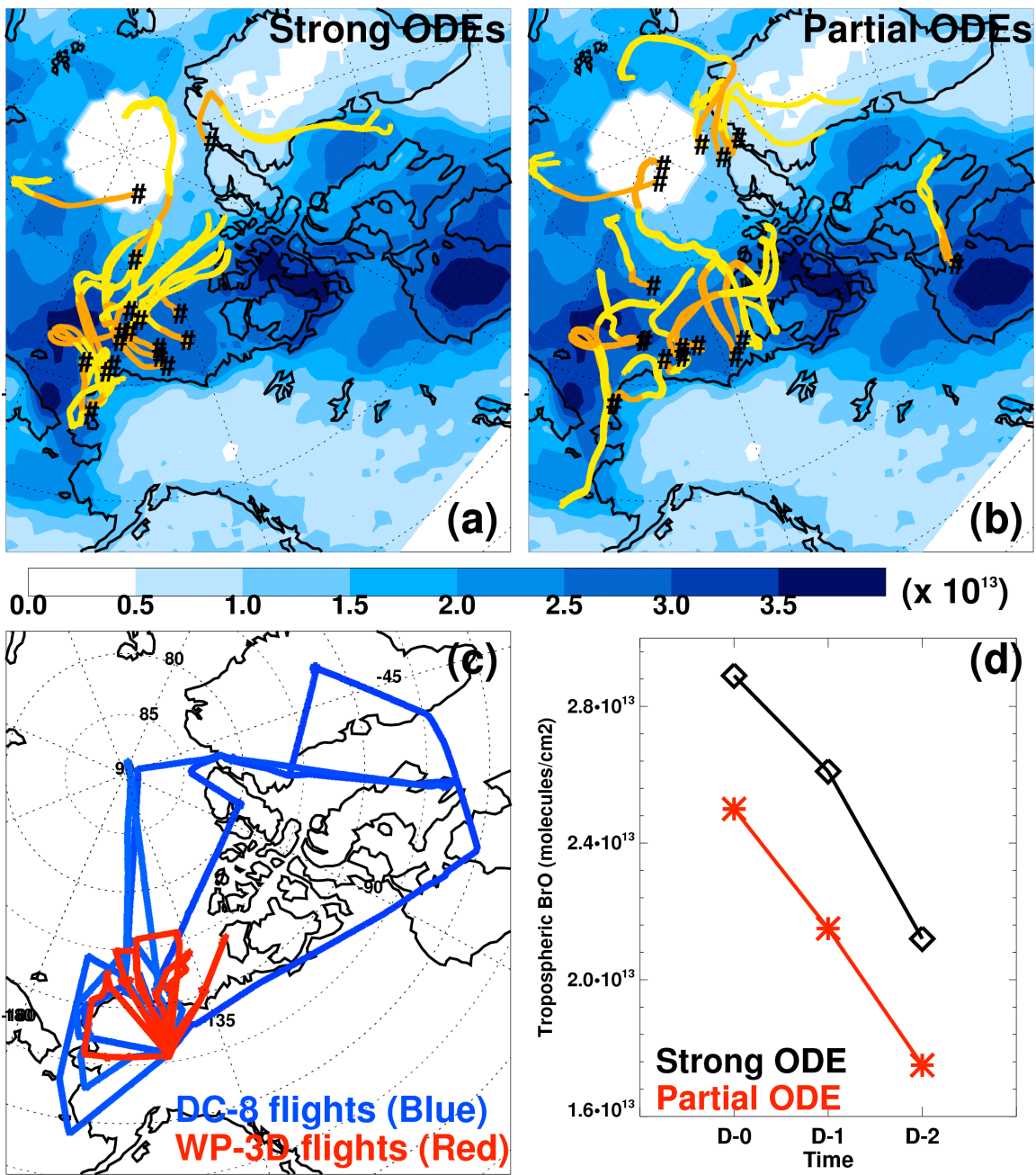
94
95
96
97
98
99
100
101
102
103

Fig. S6. Same as Fig. 2a, but for tropospheric BrO VCDs of GOME2-20th.



104
 105
 106
 107
 108
 109
 110
 111
 112

Fig. S7. Same as Fig. 5, for tropospheric BrO VCDs of OMI-SCIA2ND.



113

114

115 **Fig. S8.** Same as Fig. 5, but for tropospheric BrO VCDs of GOME2-20th.

116

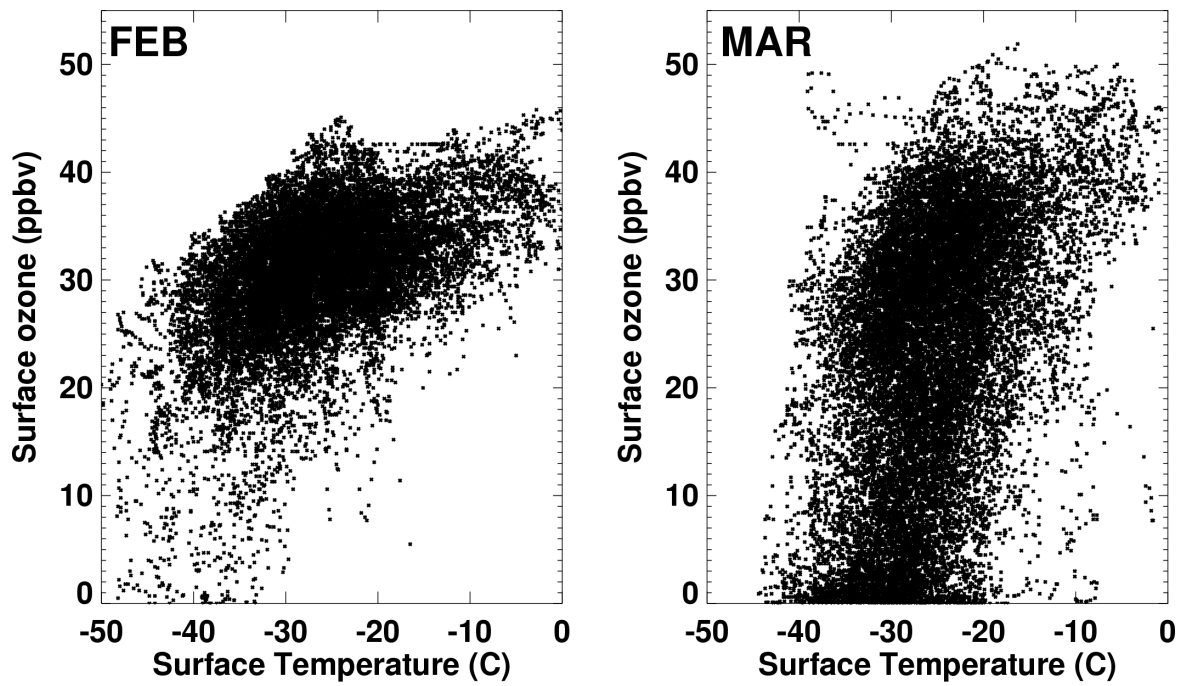
117

118

119

120

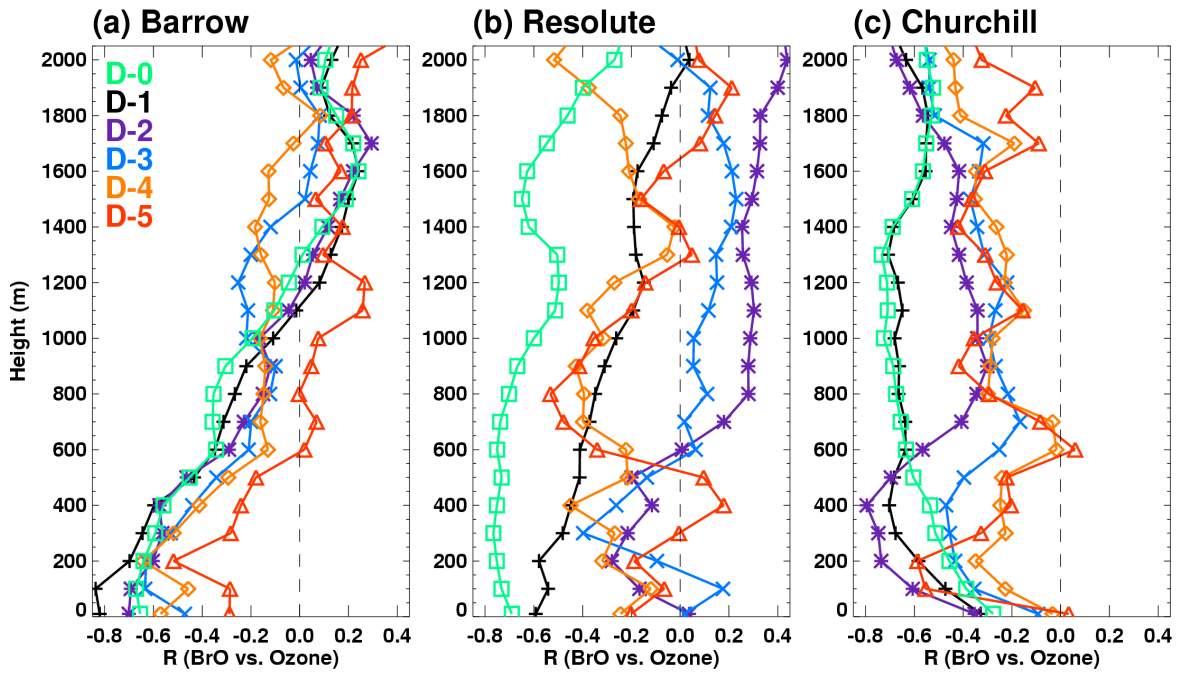
121



122
123

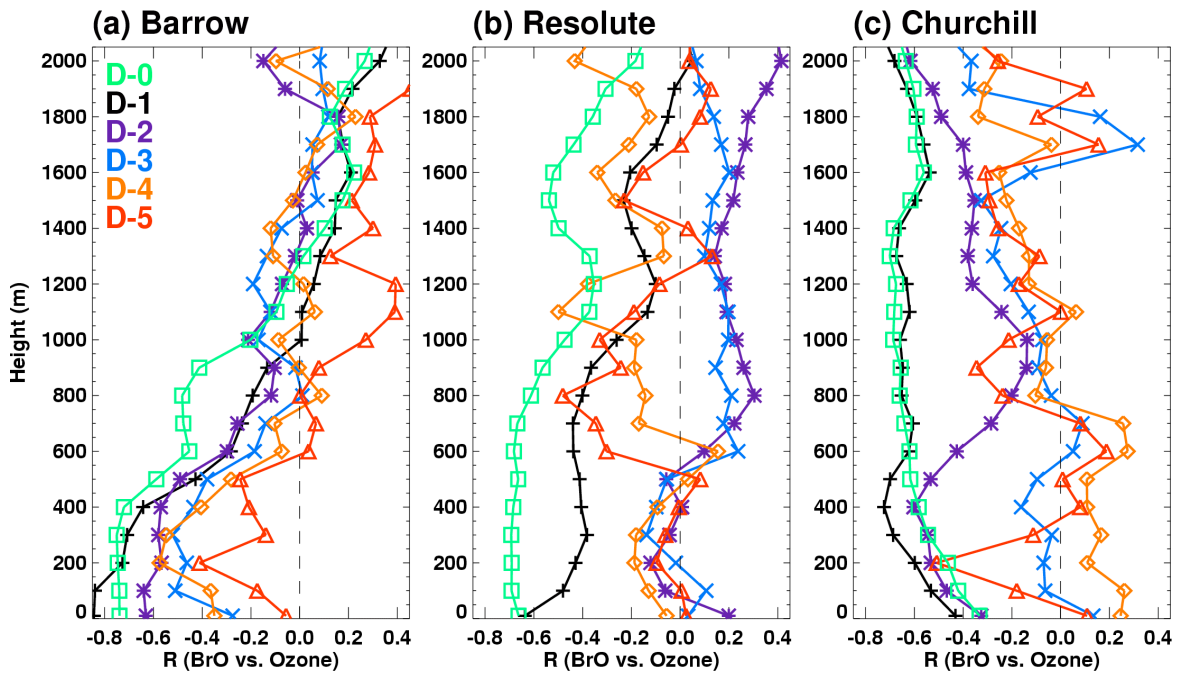
124 **Fig. S9.** Hourly surface ozone as a function of temperature at Barrow for February (left)
125 and March (right). Ozone measurements from 1979 to 2008 were obtained from the
126 NOAA Earth System Research Laboratory (ESRL) and the temperature dataset from the
127 NOAA National Climate Data Center (NCDC).

128
129
130
131
132
133
134
135
136
137
138
139
140
141
142
143
144



145
146
147
148
149

Fig. S10. Same as Fig. 9, but for tropospheric BrO VCDs of OMI-SCIA2ND.



150
151
152
153

Fig. S11. Same as Fig. 9, but for tropospheric BrO VCDs of GOME2-20th.